THE ASTROPHYSICAL JOURNAL, 412:99–110, 1993 July 20

STARBURST MODELING OF M82: TEST CASE FOR A BIASED INITIAL MASS FUNCTION

G. H. RIEKE, K. LOKEN, M. J. RIEKE, AND P. TAMBLYN
Steward Observatory, University of Arizona, Tucson, AZ 85721
Received 1992 September 28; accepted 1993 January 26

ABSTRACT

We compute starburst models for M82, making use of recent theoretical tracks of stellar evolution. Detailed comparisons of our models and those of others demonstrate this technique to be quite reliable, with relatively little change in output parameters as a function of the selection of theoretical tracks or of estimates of the observational characteristics of the stars along these tracks. The models are matched to the observational constraints for M82 summarized by McLeod et al. The rate of star formation and time of observation were thoroughly optimized to produce the most favorable fit to the observations, but we still found that the recently proposed forms for the solar-neighborhood initial mass function (IMF) cannot produce starbursts adequate to fit the observations of this galaxy. We then explored adjustments to the shape of the IMF to improve the fit to M82. We find (1) the shape of the IMF for high-mass stars need not be different from that observed locally; and (2) the most likely modification to the IMF in M82 is that stars with masses below a few $M_\odot$ form much less commonly than in the solar neighborhood.

Subject headings: galaxies: individual (M82) — galaxies: luminosity function, mass function — galaxies: starburst — stars: formation

1. INTRODUCTION

Rieke et al. (1980) (hereafter RLTLT80) showed how stellar population modeling could become an important tool in understanding starbursts such as the one in M82, even though conventional optical indicators of the population were inaccessible because of heavy interstellar extinction. Their models demonstrated that a starburst could account for the properties of the galaxy in a consistent manner and led to the prediction (since confirmed: e.g., Kronberg, Biermann, & Schwab 1985) that the galaxy would be the site of a high rate of supernova explosions. They also suggested that the star formation was biased toward more massive stars than predicted by the initial mass function (IMF) in the solar neighborhood.

There is evidence that the IMF for high-mass stars is very similar from one galaxy to another and is largely independent of environment. However, there is little if any direct evidence regarding the low-mass IMF in environments that differ strongly from the solar neighborhood. Main-sequence low-mass stars are difficult to observe even in a quiescent galaxy because of the increase in luminosity as stars of roughly solar mass ascend the giant branch. Direct observation of the low-mass IMF in a starburst galaxy is impossible, and its shape can be deduced, if at all, only indirectly. In the case of M82, RLTLT80 compared a number of observable properties of the galaxy to the predictions of starburst models. They found that these properties could not be met by models based on the solar neighborhood IMF that did not exceed a plausible fraction of the dynamical mass of the nucleus of M82. A number of specific modifications of the IMF were evaluated to show that shifting additional mass to formation of high-mass stars did allow satisfaction of the constraints. However, these specific forms were adopted only for mathematical convenience, and the conclusion reached by these authors was simply that some adjustment of the IMF toward higher masses was needed to fit M82.

M82 is ideal for applying the indirect arguments required to constrain the low-mass IMF. It is a low-mass, dwarf galaxy undergoing a very powerful starburst. As a result, the starburst output strongly dominates the output from the preexisting galaxy. As expected for a dwarf galaxy, the nuclear mass is low so that useful dynamical constraints on the mass participating in the starburst can be derived. M82 is also sufficiently close for detailed study. At the same time, the starburst in M82 appears to be typical of those occurring in other, larger galaxies. Although confirmation will be difficult in galaxies at greater distances and/or where the starburst does not so strongly dominate the total output and mass, it is plausible that conclusions about the low-mass IMF in M82 will be relevant to other starburst galaxies.

The changes that have occurred in stellar evolutionary theory since 1980 make it of interest to recalculate the models of RLTLT80 and test their arguments for a biased IMF. We have used the modern and detailed stellar tracks of Maeder & Meynet (1988, hereafter MM88) and Maeder (1992, hereafter M92) as the basis for such a test. These tracks take into account such behavior as overshooting and mass loss and provide a detailed specification of behavior in the red giant and supergiant stages, all features of stellar evolution that were treated perfunctorily in the tracks used for the previous work. The greater detail of the new stellar tracks also makes meaningful the generation of models with a broad range of input parameters.

The new models generated in this paper will be compared with a carefully updated suite of observational constraints for M82 (McLeod et al. 1993). The current work is based on the stellar behavior appropriate for solar metallicity, since the interstellar medium in M82 appears to be roughly of this metallicity (McLeod et al. 1993).

The paper is organized as follows. Section 2 describes the generation of the starburst modeling program, with emphasis on the way we translated theoretical stellar parameters into observable quantities. Section 3 compares the outputs of the new models with those obtained elsewhere and demonstrates the reliability of this technique. Section 4 discusses an extensive suite of new models of M82. The conclusions that can be drawn from these models are discussed in § 5, where we argue

that the IMF for high-mass stars can be as found in other environments, but that the formation rate for low-mass stars is relatively low in the M82 starburst. The principal results of the paper are listed in § 6.

2. GENERATION OF STARBURST MODELS

To make use of the work of MM88 and M92, we have derived observable quantities from the theoretical models. These quantities include *UBVRJHK* magnitudes, ionizing UV flux, luminosities, the strengths of the H_2O and CO stellar absorption features, supernova rates, and the yield of oxygen through nucleosynthesis. As appropriate, these quantities must be related to the stars described in the theoretical models in terms of effective temperature, luminosity, and surface gravity. The observable quantities are then combined in the starburst models in accordance with the relative numbers of stars at various evolutionary stages to predict the observable parameters of the stellar population.

We estimated *JHK* magnitudes in three different ways, described in order of priority. A partial set of magnitudes was computed with the use of the synthetic colors and magnitudes described in Bell & Gustaffson (1989) and Steiman-Cameron & Johnson (1986). These references show that these colors have a good correspondence with observation. Where these listings were incomplete, observational data found in Schmidt-Kaler (1982) and Johnson (1966) were used after normalization to the stellar tracks through comparison of effective temperatures, luminosities, and surface gravities. Finally, where extensive suites of observational data were unavailable, we estimated magnitudes from a blackbody approximation. This last resort, was needed only for massive stars of relatively high temperature for which the *JHK* magnitudes have little influence on the final outputs of the starburst models.

UBVR magnitudes were obtained from the color tables used for the isochrones of Green, Demarque, & King (1987) as described by Green (1988). These tables are based on the synthetic colors of VandenBerg & Bell (1985) and Kurucz (1979) with empirical recalibration.

The calculation of the UV fluxes for the tracks of MM88 and M92 was based on the models of Panagia (1973) in combination with those of Leitherer (1990) (there is close agreement between these two sources in the region of overlap). The UV fluxes of stars with effective temperatures lower than those discussed by Panagia (1973) were derived from the model atmospheres of Kurucz (1979). For stars with temperatures higher than those discussed by Leitherer (1990), the Zanstra method as explained by Pottasch (1984, p. 168) was inverted to calculate the UV flux. The outputs of these latter very hot stars are unimportant in modeling M82 because the ionizing spectrum is relatively soft.

Luminosities were computed as the sum of the individual stellar luminosities in the population.

The stellar CO and H_2O indices were estimated in two ways. The primary source of CO indices was the synthetic colors computed by Bell & Briley (1991). We used their calculations of CO_{CFP} for $^{12}C/^{13}C = 10$, and we reduced the calculated indices by 0.02 for the giants and dwarfs to allow for the systematic shift they found between the calculations and observational data. Comparison with observed CO indices for supergiants (Elias, Frogel, & Humphreys 1985) led us to make a similar correction by 0.05 for the modeled indices for them. Even with these corrections, the CO indices are near the maximum values that are consistent with the observations. For stellar types not included in Bell & Briley, we based the CO indices on the summaries provided by Frogel et al. (1978) and Elias et al. (1985). H_2O indices were obtained from Aaronson, Frogel, & Persson (1978).

We estimated supernova rates by assuming that every star more massive than 8 $M_\odot$ ends its evolution by exploding as a supernova. The oxygen yields per star depend on the mass of the core actually developed and therefore depend on the history of mass loss as well as on the initial mass of the star. We have used the calculations from Chiosi & Maeder (1986) to estimate these yields; these estimates are similar to the work of other investigators.

As with other programs of similar type, our starburst models are subject to oscillations caused by the discreteness in mass of the computed stellar tracks and the resulting change in model properties when switching from one mass range to another. We reduced this problem by expanding the tracks of MM88 and M92 through interpolation to include intermediate masses not listed. This interpolation was made possible by the unique property of the tracks in relating stars of neighboring masses by their corresponding stages of internal evolution. Although some oscillations are still apparent in very old starbursts (i.e., $>10^9$ yr after the episode of star formation), the outputs showed very little of this problem in the young stages of interest in modeling M82. This behavior is as expected because the computed mass intervals are cycled through rapidly for a young starburst, whereas the main-sequence time interval between computed mass intervals becomes large for old starbursts.

The interpolated stellar properties became the input data to a modified version of the population modeling code used by RLTLT80. The models generated by this code were verified in a number of experiments. To verify the operation of the code, we compared the *UBVR* outputs with the output from a stellar population code written independently by P. Tamblyn; the output of the two codes agreed to within 10%. In addition, we confirmed that the ultraviolet fluxes produced by our code were in agreement with those generated by the stellar population models computed by Leitherer (1990).

To test the dependence of the outputs on the stellar tracks, we generated a series of models from the evolutionary tracks of Bertelli et al. (1986) for comparison with the predictions from MM88 and M92. These models had an upper mass limit of 9 $M_\odot$, the largest mass considered by Bertelli et al. The two sets of theoretical calculations show somewhat different stellar behavior, particularly in the red giant stages that are important for our analysis. Nonetheless, the output predictions were very similar; as an example, Table 1 compares results for models with an IMF running from 1.3 to 9 $M_\odot$ and in which the number of stars per logarithmic mass interval is a power law with an index of 1.5. The star formation rate (SFR) is exponential with a time constant of 2×10^7 yr, and the population is observed 3×10^7 yr from the initiation of the burst. The models were normalized to a mass of 2.5×10^8 $M_\odot$.

TABLE 1

COMPARISON OF STARBURST MODELS

Model	Luminosity ($L_\odot$)	M_K
MM88	1.2×10^{10}	−18.5
M92	1.2×10^{10}	−18.5
Bertelli et al. 1986	1.2×10^{10}	−18.4

3. MODELING OF M82: COMPARISONS WITH OTHER MODELS

3.1. *Models of RLTLT80*

We have compared the updated starburst models with those calculated by RLTLT80, as shown in Table 2 (the IMFs are listed as A through I in Table 5). The input parameters and basic operation of the computer code are exactly the same for the two sets of models, so comparing the model results with those in the previous paper allows one to determine the changes resulting from improvements in stellar evolutionary theory and the corresponding observational parameters. In general, the results are similar, and conclusions based on the previous models are likely to be supported by the new ones. A detailed comparison does reveal differences, however, which we discuss in turn below. In making these comparisons, recall that oscillations were not suppressed by interpolation between tracks in the older models; combined with the sparseness of points along these tracks, some problems with oscillations would be expected in the predictions of the old models. We expect that some of the scatter in the comparisons has this origin.

Luminosity.—A review of the earlier models has discovered a numerical error by a factor of 2 in the luminosities. This error has been corrected in the values entered in Table 2. The agreement between new and old models is then reasonably close, with a systematic trend for the old models to give higher luminosities where the shape of the IMF allows substantial numbers of intermediate-mass stars (3–8 $M_\odot$) and lower ones where the IMFs are heavily weighted to stars more massive than this range. The models based on M92 give luminosities systematically lower than those based on MM88 by a factor of 1.2–1.4.

K-Magnitude.—Results of the new models are generally similar to those of RLTLT80, with the new models tending to be fainter at K than the old ones. The largest differences occur for models biased toward massive stars and at old ages, where models based on M92 can be 4 times fainter than the 1980 models. In contrast, where less massive stars and young ages are emphasized, the new tracks yield K brightnesses very similar to the 1980 ones, in some cases even slightly brighter than the old models. Models based on M92 are systematically slightly fainter than those using MM88. The discrepancies between new and old models probably arise because of the much greater detail in specifying the red giant evolution in the new models, where typically more than 20 evolutionary steps are calculated. Many of the old stellar tracks included only a single red giant point.

UV Fluxes.—The new models predict ionizing fluxes roughly the same to about 4 times lower than those from the old models. M92 predictions are very similar to those using MM88. Note, however, that the MM88 tracks lead to relatively high outputs of UV flux compared with models based on tracks generated by other authors (R. C. Kennicutt, private communication).

The reasonably good agreement between the new models and the old ones reinforces our findings in comparing models based on MM88 and M92 with those from the tracks of Bertelli et al. (1986). That is, the starburst modeling appears to give results that are only modestly dependent on the existing level of uncertainty in theoretical stellar evolutionary tracks and observational parameters.

Where differences exist between the new and old models, they are often in the direction that the newer models tend to

TABLE 2

COMPARISON OF MODELS OF M82 WITH THOSE OF RLTLT80

Model	L (10^{10} $L_\odot$)	M (10^8 $M_\odot$)	M_K	log (UV)	t_0 (10^7 yr)	Age (10^7 yr)
Mod A	2.3	3	−21.5	53.1	2	3
MM88	4.0	3	−22.2	53.1	2	3
M92	3.2	3	−21.9	53.0	2	3
Mod B	3.6	3	−22.8	53.4	2	5
MM88	5.3	3	−22.8	53.2	2	5
M92	3.9	3	−22.3	53.2	2	5
Mod C	4.9	1.6	−23	53.7	2	6
MM88	2.8	1.6	−22.1	53.2	2	6
M92	2.0	1.6	−21.6	53.1	2	6
Mod D	4.4	1.8	−23	53.5	2	5
MM88	4.6	1.8	−22.6	53.2	2	5
M92	3.4	1.8	−22.2	53.1	2	5
Mod E	3.9	2.5	−23	53.0	2	5
MM88	5.6	2.5	−22.7	52.9	2	5
M92	4.3	2.5	−22.4	52.9	2	5
Mod F	2.7	2.3	−23	53.3	10	16
MM88	2.1	2.3	−22.0	52.9	10	16
M92	1.5	2.3	−21.4	52.9	10	16
Mod G	7	0.8	−23	53.9	2	3
MM88	5.4	0.8	−22.8	53.5	2	3
M92	4.0	0.8	−22.4	53.4	2	3
Mod H	8.5	3	−22.8	53.2	2	2.5
MM88	12	3	−23.1	53.1	2	2.5
M92	10	3	−23.1	53.0	2	2.5
Mod I	5	2.1	−23	53.3	5	5
MM88	5.7	2.1	−22.7	53.0	5	5
M92	4.5	2.1	−22.4	52.9	5	5

reduce the output per unit mass of forming stars. Therefore, given the same observational constraints and theoretical assumptions, the new models would not modify the conclusions reached by RLTLT80.

The new models to be described below test these conclusions thoroughly by relaxing a number of assumptions in RLTLT80. In the earlier work, the star formation was assumed to start abruptly and to decay exponentially. In the new calculations, we found that models that assumed a double burst of star formation allowed us to come closer to meeting a given set of observational constraints than RLTLT80 could with single exponential bursts. In addition, the older work imposed the upper limit on the temperature of the ionizing field by a truncation of the IMF toward high-mass stars (a simplification adopted for convenience, since detailed stellar tracks were not readily available for masses above 31 $M_\odot$). In the new work, we have assumed that the IMF extends up to 80 $M_\odot$ and have determined the portion of the UV flux generated by stars hotter than 40,000 K. Bursts are required to age until this hot ionizing flux is no more than 25% of the total ionizing flux, which is the limit derived by McLeod et al. (1993) for consistency with the observed emission-line spectrum. Of course, the new models utilize the newer stellar evolutionary tracks and the extensive interpolation to suppress oscillations, as has already been discussed.

3.2. *Models by Bernlohr*

Bernlohr (1992) has recently reported starburst models of M82 and decides that a modification of the IMF similar to that suggested by RLTLT80 is required to fit the observational constraints. His work is in parallel and independent of ours and has a number of similarities and differences. He has used stellar evolutionary tracks from a variety of sources, but from his Table 1 we conclude that his calculations should be most closely comparable with our MM88 models. Like us, he has interpolated between similar evolutionary stages to smooth out oscillations, although his interpolation was linear whereas we used a combination of polynomial and linear interpolation. Bernlohr's computer code synthesized the starburst characteristics via Monte Carlo techniques. Most importantly, he used different sources for the observational parameters associated with the stellar tracks. For example, the broad-band photometric colors were derived from the observational data summarized by Schmidt-Kaler (1982) and Flower (1977), an approach we utilized only in the minority of cases where convolutions of the photometric bands with atmospheric models were unavailable from the literature. Similarly, his estimates of the CO indices were derived from observational data, which were a secondary source for our work. To estimate the UV outputs, Bernlohr used the Kurucz (1979) model atmospheres whereas we used the analyses by Panagia (1973) and Leitherer (1990).

Because of these differences, comparison of our models with those of Bernlohr gives an overview of uncertainties in both studies associated with the starburst codes and with the assignment of stellar properties. Bernlohr compared his results with those of RLTLT80; two corrections are, however, required in his comparison. First, he normalized on the luminosity of the burst, which as we discuss above is a factor of 2 too high in the RLTLT80 models. Second, he compared only the mass in luminous stars with the masses tabulated by RLTLT80; however, the earlier reference listed the *total* masses converted into stars in the models. Table 3 gives a corrected comparison, which includes the parameters which we will show below are most important in constraining the starburst conditions.

TABLE 3

COMPARISON OF MODELS OF M82 WITH THOSE OF BERNLOHR

Model	L (10^{10} $M_\odot$)	M_K	log (UV)	CO
Mod A				
MM88	4.0	−22.2	53.1	0.26
Bernlohr	5.3	−22.6	53.2	0.21
Mod B				
MM88	5.3	−22.8	53.2	0.24
Bernlohr	6.0	−22.9	53.3	0.19
Mod C				
MM88	2.8	−22.1	53.2	0.23
Bernlohr	3.0	−22.2	53.3	0.20
Mod G				
MM88	5.5	−22.8	53.5	0.26
Bernlohr	7.0	−23.0	53.6	0.22

The two sets of models are gratifyingly close in predicted outputs, with typical differences of the order of only 20%–30%. We note that Bernlohr's predicted CO indices are about 0.04 smaller than ours, a difference that is within the probable calibration uncertainties but which also emphasizes that we have adopted values that are as large as are permitted by the observational data. Bernlohr investigated starburst models with differing metallicity and found that the changes in composite output parameters were small except for the expected dependence of CO index.

Both our new models discussed below and those of Bernlohr (1992) use modern evolutionary tracks. However, his models assumed single starbursts with an instantaneous start and stop and a constant rate of star formation in between. To avoid overproducing metals, he imposed an upper mass limit on his IMFs in the range 30–50 $M_\odot$. Therefore, Bernlohr's theoretical assumptions were very similar to those of RLTLT80; as discussed with regard to the models of RLTLT80, our new models remove these assumptions and therefore test the conclusions about the IMF more thoroughly. In addition, Bernlohr used observational constraints drawn from various sources, many of which need revision in light of more recent data. For example, two of his four "successful" models fail to satisfy the lower limit to the output at 2 μm.

3.3. *Models of Doane and Mathews*

Doane & Mathews (1993) have constructed models that are constrained primarily by the supernova rate and the dynamical mass. They also find that an IMF with a bias toward massive stars is required to explain the current supernova rate without violating the mass constraints. Their treatment is based on a number of simplifying assumptions, and they do not carry out the detailed optimization of the rate of star formation that we report below. Nonetheless, their treatment is important because it emphasizes the importance of the supernova rate alone in providing insight to the IMF in M82.

4. ADDITIONAL MODELING OF M82

To utilize the modern stellar tracks to reexamine the conclusions reached by RLTLT80, particularly those involving the necessity for an IMF biased toward high masses, we have carried out a series of efforts. First, as discussed in an accompanying paper (McLeod et al. 1993), we have redetermined the

TABLE 4

OBSERVATIONAL CONSTRAINTS ON M82 STARBURST MODELS

Date	L (10^{10} $L_\odot$)	M (10^8 $M_\odot$)	M_K	H_2O	CO	log UV	M_u ($M_\odot$)	Fe/H	SNR (yr^{-1})
1980.....	4.0	3.0	−23.0	...	...	53.3	31	...	...
1992.....	>5.0	<2.5	< −22.5	<0.06	>0.21	>54.0	[a]	Solar	~0.1

[a] No more than 25% of the ionizing flux from stars hotter than 40,000 K.

observational constraints appropriate to starburst models of M82, which we summarize in Table 4. Second, we have adjusted the time dependence of star formation to provide the closest possible fits to these observational constraints. This optimization takes advantage of the detail of the stellar tracks from M92. The optimum SFR(t) differs significantly from those used both by RLTLT80 and by Bernlohr (1992); thus, both of these studies may be pessimistic with regard to a given IMF being able to satisfy a suite of observational constraints. Third, we have constructed models in which the IMF is extended to large stellar masses and have let the aging of the population result in the required softening of the radiation field to fit the emission-line spectrum. Combined with our conclusion that a significant portion of the gas may be excited by stars hotter than 40,000 K, this approach again should make it easier to fit the observational constraints than with the models of RLTLT80 and Bernlohr, both of which assumed IMFs with upper mass limits near 30–40 $M_\odot$.

As indicated in Table 4 and discussed in McLeod et al. (1993), many of the listed constraints are actually lower (or upper) limits that make the least possible demands on the starburst models. We therefore expect a fully satisfactory model to satisfy these limits with ease to allow some latitude, for example, for the absorption of UV photons by dust and for the presence of regions optically thick at 2 μm that would not be included in the estimate of the absolute K-magnitude. A constraint we have not listed in Table 4 is that the time of observation must be late enough in the starburst for supernovae to drive the observed X-ray wind out of the galaxy. We have set the X-ray timing constraint by assuming that the wind starts as soon as the supernova rate exceeds 0.01 yr^{-1} and that it requires at least 1×10^7 yr to expand to the observed distance of 8 kpc (McLeod et al. 1993).

The deep CO bands in M82 provide an important constraint. These features become stronger as the stellar temperature is decreased, as the surface gravity is decreased, and as the metallicity is increased. It has been suggested (e.g., Lester et al. 1990; Gaffney & Lester 1992) that the deep bands in M82 may arise from high metallicity in red giant stars rather than from the surface gravity dependence in a spectrum dominated by red supergiants. We have evaluated this possibility by running the full set of models discussed below but with the CO band strength saturated at the maximum level found for giants of a given spectral type, i.e., CO band strengths appropriate for stars with $\log g < 1.50$ were set to the values for $\log g = 1.50$. The most favorable models fell short of fitting the observed CO index by at least 0.03 on the nucleus and 0.06 on the position 8″ west and 2″ south of the nucleus. Extrapolating the dependence of CO index on metallicity reported for the starburst models of Bernlohr (1992), minimum metallicities of greater than 3 and greater than 10 times solar would be required respectively in the nuclear and the off-nuclear positions. Both of these values substantially exceed the current metallicity of the interstellar medium out of which these stars formed (presumably the metallicity was lower when they formed than it is now). Therefore, the deep CO bands require that the spectrum be dominated by red supergiants.

Figure 1 shows the output of a starburst model in a form that will be used for the remainder of the discussion in this paper. The SFR has been assumed to be Gaussian in time, with a full width at half-maximum (FWHM) of 5×10^6 yr. The peak rate occurs at 5×10^6 yr. Stars are assumed to form according to an IMF that is a piecewise power-law approximation to the local IMF proposed by Miller & Scalo (1979), as described by IMF 1 of Table 5. As in RLTLT80, we have adopted a different approximation to the Miller & Scalo IMF than they suggested; our approximation increases the proportion of high-mass stars while still remaining a reasonably good fit. Stars form on the zero-age main sequence in accordance with this mass function and with the Gaussian time dependence with the requirement that a total of 2.5×10^8 $M_\odot$ of stars will have formed by t = infinity. The graph shows the total luminosity (L), the ionizing photon flux (UV), the absolute K-magnitude (K), the CO index (CO), and the portion of UV flux generated by stars hotter than 40,000 K (T[UV]) as a function of time from the beginning of the starburst. Output parameters that did not constrain the models strongly have not been plotted (the metal abundance and supernova rates will be discussed later). The output parameters of the model have been normalized to the observational constraints for M82 listed in Table 4, so that a successful model would have all the plotted data at or above a value of 1. Because our constraints are usually in the form of limits, values significantly above 1 are not considered a drawback. The timing constraint imposed by the extent of the X-ray wind is indicated by the vertical line near 13 million yr. Acceptable models should satisfy the other observations after the timing constraint is satisfied, i.e., their outputs should all lie in the shaded portion of Figure 1.

It can be seen that the ultraviolet flux peaks early in the starburst and fades quickly, falling below the target value while

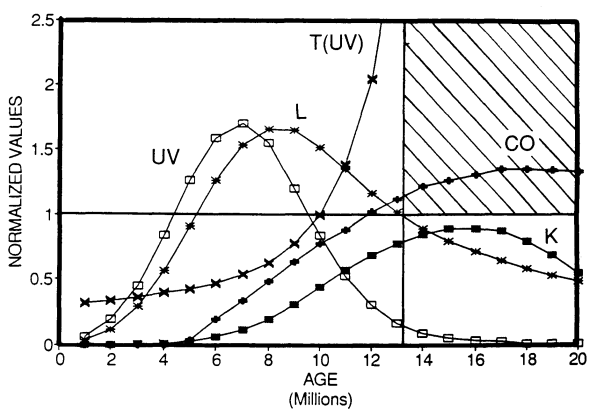

FIG. 1.—Output of a single Gaussian starburst using the Miller & Scalo (1979) IMF (IMF 1).

TABLE 5

SUMMARY OF IMF PARAMETERS

IMF	m_1	α_1	m_{*1}	α_2	m_{*2}	α_3	m_u
A[a]	0.09	0.25	1	1.5	10	2	31
B	1.25	1	...	...	...	...	31
C	3.5	0	...	...	...	...	31
D	3.5	1	...	...	...	...	31
E	3.5	2	...	...	...	...	31
F	3.5	1	...	...	...	...	31
G	8.0	1	...	...	...	...	31
H	3.5	1	...	...	...	...	16
I	3.5	1	...	...	...	...	20
1[a]	0.1	0.25	1	1.5	10	2	80
2[b]	0.1	0.25	1	2	...	...	80
3[c]	0.1	0.25	0.56	1.7	...	...	80
4	0.1	0.25	1	1.5	...	...	80
5	0.1	0.25	1	1.5	10	1	80
6	0.1	0.25	3	1.5	...	...	80
7	0.1	0.25	6	1.5	...	...	80
8	0.1	0.25	3	1.5	10	2	80
9	0.1	0.25	6	1.5	10	2	80
10	0.1	0.25	3	2	...	...	80
11	0.1	0.25	6	2	...	...	80

[a] Miller & Scalo 1979; Rana 1987.
[b] Scalo 1986.
[c] Basu & Rana 1992.

the flux at K and the CO index are both well below the observed values. The K flux peaks as the massive stars evolve into red supergiants, reaching nearly the minimum output required for M82 after the UV has faded far below the required value. The luminosity peaks at a time intermediate between the maximum UV and K fluxes. There is no time when all of the observational constraints come close to being satisfied. A specific problem is that the ultraviolet output for a single short burst has faded far below the target value when the X-ray timing constraint has been met.

We adjusted the time dependence of the SFR to improve the fit to the observations. After experimentation with exponential SFRs, multiple exponentials, and constant SFRs, we found that the most favorable time dependence for the SFR was to have two short bursts. The first burst is required to provide the supernovae that start the wind of hot gas observed in the X-ray and to provide the red supergiant stars seen in the near-infrared. The second burst is needed to supply the ultraviolet flux. Because the time constraints imposed by the X-ray wind and by the growth of the red giant branch are similar, no further optimization of the rate of star formation could improve the fitting to the constraints. Lengthening the bursts did not improve this fitting since it tended to broaden and reduce the peaks in the outputs of the stellar population and made it more difficult for these parameters to reach the values observed in M82.

We therefore ran a set of models with two bursts with SFRs that were Gaussian in time with a FWHM of 5×10^6 yr and consumed a total of $2.5 \times 10^8\ M_\odot$. We adjusted (1) the relative masses of the bursts; (2) the time interval between them; and (3) the time of observation to provide the closest possible fit to the parameters of M82. Since our experiments confirmed that all other forms for the rate of star formation produced poorer fits to the observations, the models discussed below should represent a "best case" for fitting these constraints. That is, any other forms for the SFR would be expected to have greater difficulty in satisfying the constraints than the models we present below.

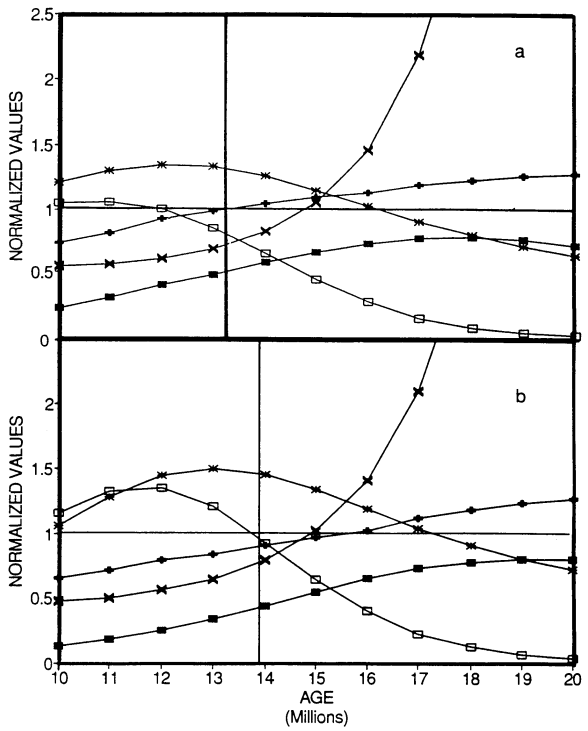

FIG. 2.—Two optimized double starbursts for M82 using IMF 1. In (*a*), the available mass is divided equally between the bursts, and the best match to the observational constraints occurs with a delay between bursts of 5 million yr with the observations at 10 million yr after the first burst. In (*b*), $\frac{1}{4}$ of the available mass is in the first burst; the optimized values of the other parameters are similar to (*a*).

Figure 2 summarizes our calculations for IMFs similar to that of Miller & Scalo (1979) as approximated by IMF 1 of Table 5. Six models were run, varying the portion of the mass in the initial burst and the time interval between bursts over the ranges that came closest to fitting the observational constraints. As illustrated by the sample starbursts in the figure, satisfying the UV flux and X-ray timing constraints required virtually all of the mass to be converted into stars in the second burst, but doing so resulted in inadequate output at K (and somewhat weak CO bands) during the period when the UV fluxes came close to the requirements. If we define the optimum fit as the time when the UV field first becomes cool enough, either the UV or the K flux (and usually both) is short by about a factor of 2. Even with the additional degree of freedom allowed by multiple bursts of star formation, these results are in agreement with the conclusion by RLTLT80 that this form of IMF is incompatible with the observations of M82.

We have considered a number of additional estimates of the local IMF. The IMF found by Rana (1987) falls close enough to that of Miller & Scalo (1979) that the same approximation used for Figure 2 is appropriate for it, so we reach the same conclusions. The IMF estimated by Scalo (1986) falls more steeply toward high masses as indicated by IMF 2 of Table 5. The starburst models for this case are summarized in Figure 3. Eight cases were run, varying the relative amounts of mass in the two bursts and the time interval between them. Models with small initial bursts fell short in both near-infrared and UV flux (by factors of 4–5) and those with large initial bursts fell short in the near-infrared by a smaller factor (about 3) and in the UV by a larger one (more than 20). As indicated in the

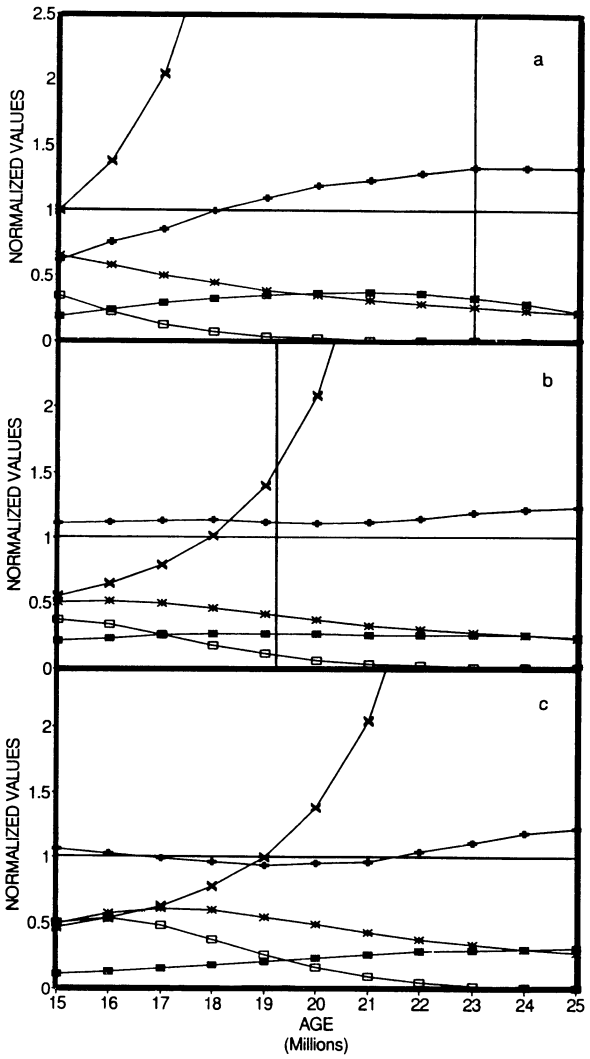

FIG. 3.—Starbursts for M82 using Scalo (1986) IMF (IMF 2). (*a*) shows the output from a single burst; (*b*) shows an optimized double burst for $\frac{1}{2}$ of the available mass in the initial burst and 8 million yr between bursts; (*c*) has $\frac{1}{4}$ of the available mass in the initial burst and 9 million yr between bursts.

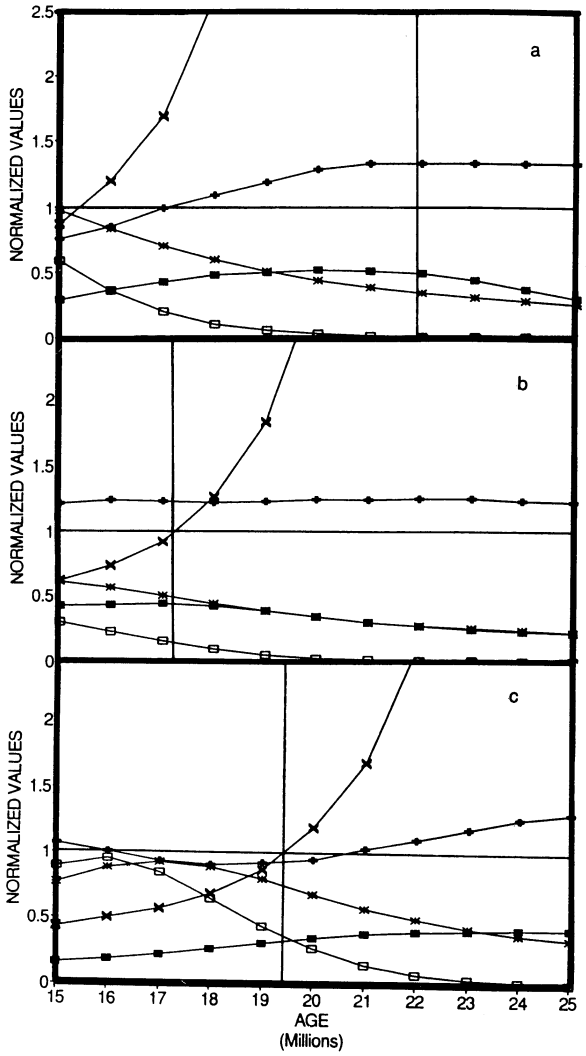

FIG. 4.—Starbursts for M82 based on Basu & Rana (1992) IMFs as represented by IMF 3. (*a*) shows a single burst; (*b*) has 75% of the mass in the initial burst and 7 million yr between bursts; (*c*) has 25% of the mass in the first burst and 9 million yr between bursts.

figure, the relatively low supernova rate places the X-ray timing constraint relatively late, but we found that delaying the second burst in proportion allowed fits as close as could have been achieved without this delay. Again, this form of IMF is not compatible with the observations of M82. IMF 3 is a reasonably good fit to three possible forms of the IMF considered by Basu & Rana (1992), namely those characterized by $\tau = \infty$, $\tau = 15$ Gyr, and $\tau = -15$ Gyr, where τ is the time scale for star formation (and negative values indicate increasing star formation with time). Figure 4 illustrates three of seven models run with this IMF; the shortfalls relative to the target values are large, similar to those using IMF 2.

The overriding problem in fitting M82 with the local IMFs discussed above is that most of the newly formed stars are of low mass and hence do not contribute significant luminosity at the ages of interest. Therefore, improvements in the fits require that some of the mass in low-mass stars with these IMFs be shifted into intermediate- and high-mass stars so that there is a greater efficiency in converting the observed dynamical mass into luminosity at ages of 10^7 to a few times 10^7 yr. A variety of models with such modifications is described below.

Figure 5 shows an example of a series of models similar to those in Figure 2, except that the IMF is not allowed to steepen toward very high masses. The functional form is given in Table 5 as IMF 4. Thirty-nine models were run for this IMF, again varying the relative amounts of mass for the two bursts and the time interval between them. The results for a single burst and the most favorable double burst case are illustrated. The former case has the expected difficulty of the UV flux falling much too low by the time the X-ray timing constraint has been met. In the latter case, all the observational constraints are nearly satisfied for an interval between bursts of 8 million yr, 15% of the mass in the first burst, and the time of observation 13–14 million yr after the peak of the first burst (i.e., 18–19 million yr on our time scale). However, most of the constraints are barely met (and the CO index and *K*-flux constraints are not quite satisfied), so any deviation of the SFR from the strict double burst we have assumed would immediately produce shortfalls in most parameters. Nonetheless, the improvement relative to the local IMF models is striking.

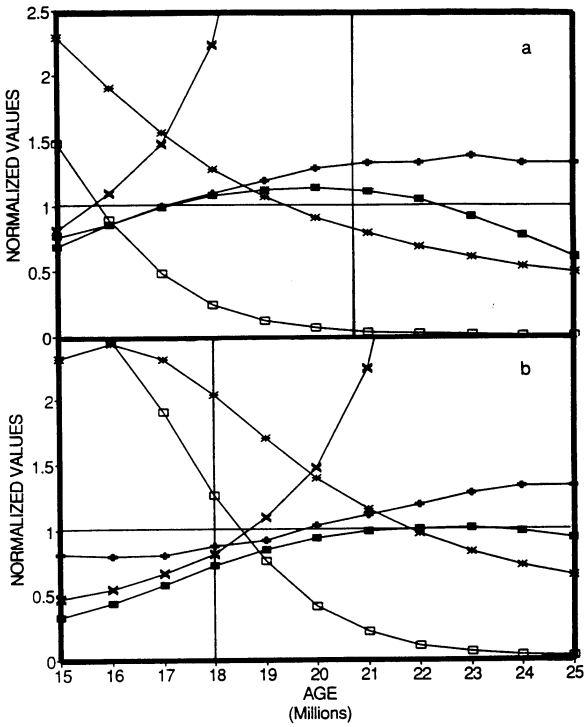

FIG. 5.—Starbursts for M82 with additional high-mass stars through IMF 4. (*a*) shows the output from a single burst; (*b*) shows the output from an optimized double burst, which has 15% of the available mass in the first burst and a time delay of 8 million yr between bursts.

IMF 4 is a good fit for the fourth possible form for the local IMF considered by Basu & Rana (1992), that for $\tau = 5$ Gyr. However, they note that time scales as short as this value for the rate of star formation predict higher rates of formation of white dwarfs and neutron stars than are observed, and therefore they conclude that the cases represented by IMF 3 are more accurate representations of the local IMF. The fact that IMF 4 predicts a higher portion of high-mass stars than is compatible with the number of white dwarfs and neutron stars in the local neighborhood and still is unable fully to satisfy the constraints emphasizes the difficulties in meeting these constraints with local-type IMFs.

IMF 5 increases the portion of high-mass stars still further by decreasing the slope above 10 $M_\odot$. This case allows a slightly stronger initial burst since less mass is required to generate the UV. An example is shown in Figure 6. Although this case produces only a modest improvement over the cases illustrated in Figure 5, it does meet all the constraints.

Increasing the proportion of very high mass stars in the calculations above only produced modest improvements, so we next examined the consequences of changing the inflection in the IMF at 1 $M_\odot$ to higher values of mass. Such a modification tends to increase the portion of intermediate- and high-mass stars, with a substantial reduction in the number of low-mass ones. Seven cases were run for each of IMFs 6 and 7 of Table 5 (i.e., similar to the models of Fig. 5 except with inflection points at 3 and 6 $M_\odot$). Figure 7 shows two of the most favorable cases; increasing the inflection mass allows fits to the observational constraints with a significant margin.

These runs showed a large output in the near-infrared at ages of about 30 million yr due to the increase in the number of intermediate-mass stars at the extreme tip of the asymptotic

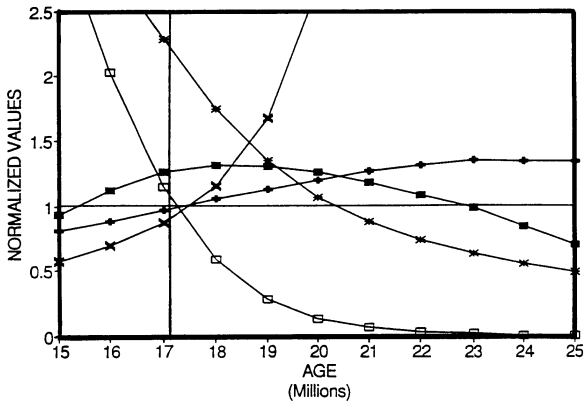

FIG. 6.—Result of a further increase in the number of high-mass stars through IMF 5. 25% of the mass is in the initial burst and the interval between bursts is 5 million yr.

giant branch. Seven models each were run with IMFs 6 and 7 with second bursts timed to coincide with this near-infrared peak emission and to provide the necessary UV flux. As shown in Figure 8, the most favorable of these models were able to fit all the constraints.

The fits achieved at ~35 million yr in Figure 8 are possible only because of the enhancement of intermediate-mass stars relative to local-type IMFs. Figure 9 illustrates this point by showing models similar to those in Figure 8 but using the most favorable local-type IMF, IMF 1. The shortfalls in this age range are larger than with the same IMF with a shorter interval between bursts, as illustrated in Figure 2.

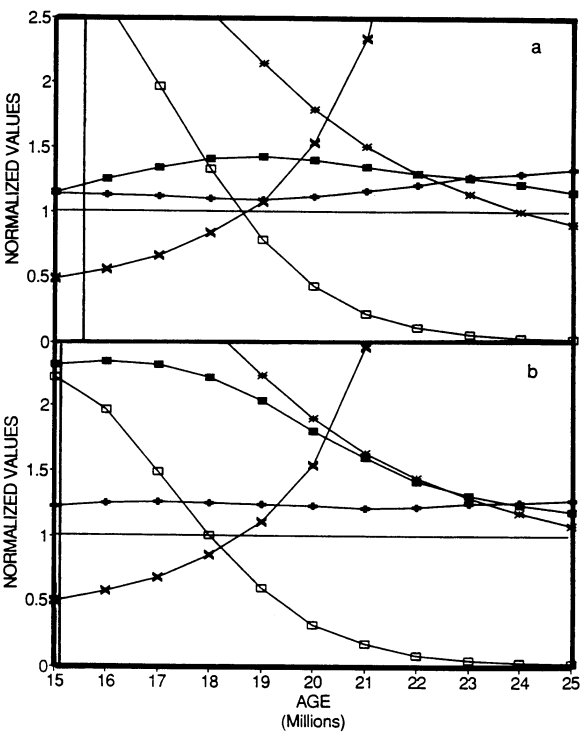

FIG. 7.—Starbursts for M82 with additional high- and intermediate-mass stars through IMFs 6 and 7. (*a*) shows a double burst with $\frac{1}{2}$ the available mass in the first burst, m_{*1} at 3 $M_\odot$, and a time interval of 8 million yr between bursts; (*b*) shows a similar double burst except that 75% of the available mass is in the first burst and $m_{*1} = 6\ M_\odot$.

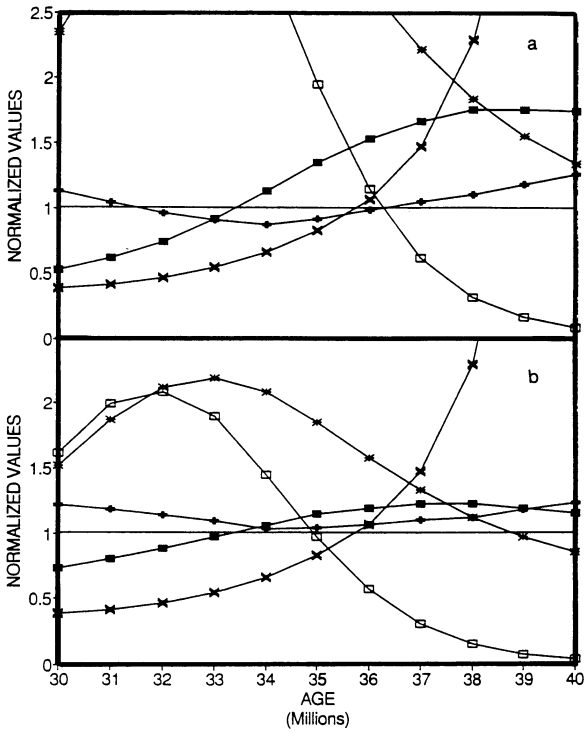

FIG. 8.—Models as in Fig. 7*b*, except the time between bursts is 25 million yr. (*a*) has 50% of the mass in the initial burst and (*b*) has 75%.

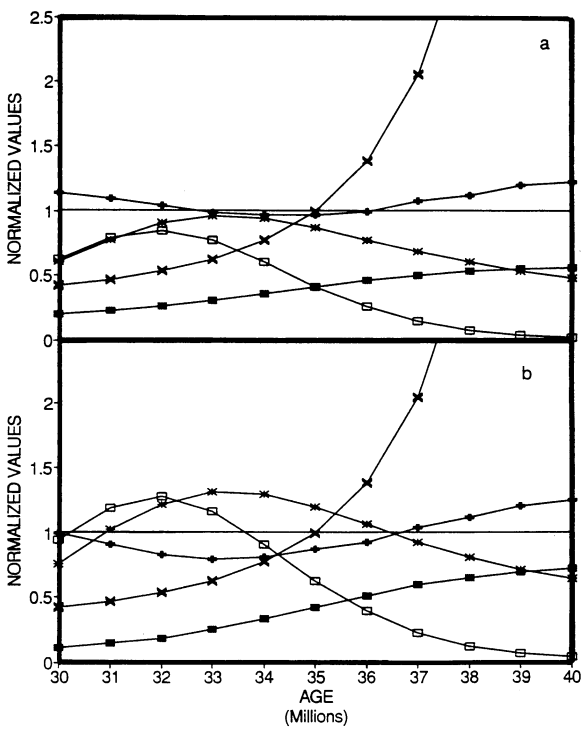

FIG. 9.—Models using IMF 1 and with 25 million yr between bursts. (*a*) has 50% of the mass in the initial burst and (*b*) has 25%.

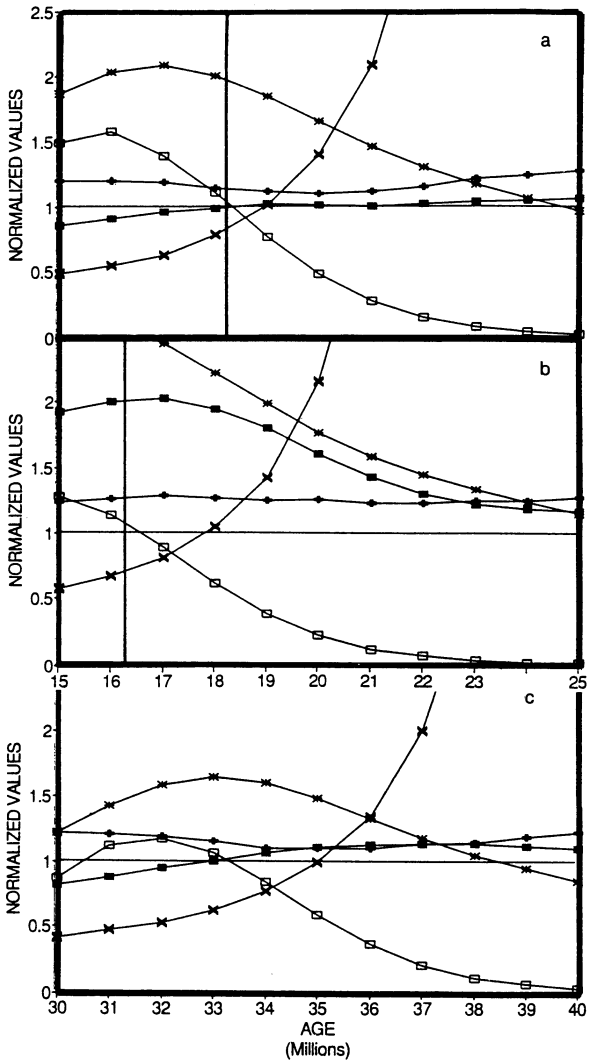

FIG. 10.—Models with the shape of the high-mass IMF from Miller & Scalo (1979). (*a*) uses IMF 8 and has 50% of the mass in the first burst and 9 million yr between bursts; (*b*) uses IMF 9 and has 75% of the mass in the initial burst and 8 million yr between bursts; (*c*) is similar to (*b*) except there are 25 million yr between bursts.

Of the models discussed so far, the most satisfactory fits were obtained with ones such as those in Figures 7 and 8, where the inflection point in the IMF is moved up from 1 $M_{\odot}$, and the relative number of very high mass stars is increased slightly by modifying the power-law slope of the IMF. Figure 10 explores which type of change in the IMF is the most important by setting the slope of the IMF at high masses back toward that for the local stellar population; see IMFs 8 and 9. Comparing with Figure 7, it can be seen that the comparisons with observation are nearly as good if we increase only the mass of the inflection of the IMF and leave the high mass IMF similar to that of Miller & Scalo (1979). As shown in Figure 11, the discrepancy with observation is increased with IMFs 10 and 11, where we have taken the high-mass segment to be similar to the local IMF of Scalo (1986). However, even in these cases a more radical reduction in the proportion of low-mass stars would provide an adequate fit.

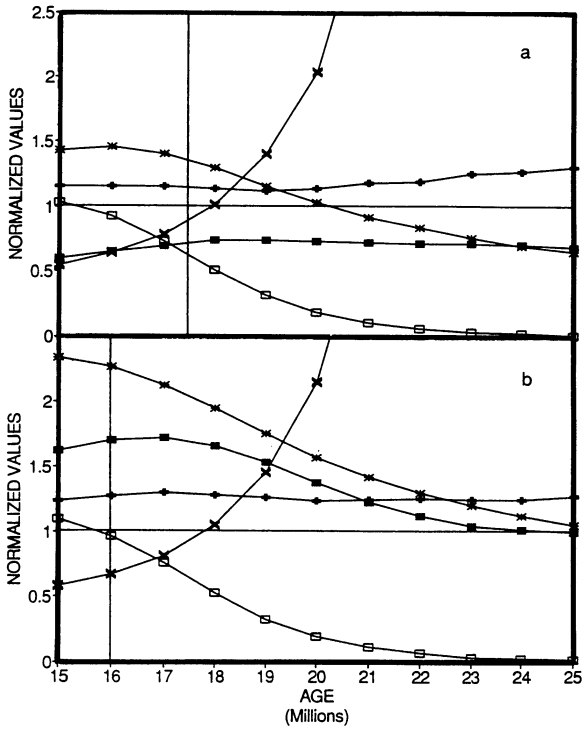

FIG. 11.—Models as in Fig. 7*a* and 7*b*, but with the shape of the high-mass IMF from Scalo (1986). (*a*) uses IMF 10 and (*b*) uses IMF 11.

5. DISCUSSION

From the analysis above, we conclude that the observations of M82 require IMFs that suppress the formation of low-mass stars relative to the forms deduced for the local neighborhood, but that the high-mass portion of the M82 IMF can be similar to that observed locally. Alternately, IMFs that significantly increase the proportion of very massive stars can meet the constraints. We have also found that IMFs of the first kind that emphasize the intermediate-mass range can satisfy the observational constraints in two ways: (1) two closely spaced bursts, with the time of observation about 13 million yr after the first burst; and (2) two bursts separated by about 25 million yr with the time of observation about 30 million yr after the first burst.

This section begins by considering two additional constraints. We then summarize the information on the IMF that can be deduced from all the observational constraints together.

5.1. *Abundances and Supernova Rates*

Rieke (1989) pointed out that the existing starburst models predicted the formation of large amounts of metals, particularly oxygen, because of the extensive processing in very high mass stars and the high star formation efficiency, which leaves relatively little unprocessed interstellar medium (ISM) to dilute the supernova ejecta. Bernlohr (1992) found the generation of high metallicity a troublesome problem with his models, which led him to truncate the IMFs at high stellar masses.

Oxygen is a useful element to study in this regard, both because the far-infrared observations of fine structure lines constrain the amount of oxygen directly (Duffy et al. 1987; McLeod et al. 1993) and because the yield of oxygen is fundamental to the processes occurring in evolved high-mass stars and its production is well understood since the work of Arnett (1978).

TABLE 6

OXYGEN YIELDS AND SN RATES

IMF	Oxygen ($10^6\ M_\odot$)	SNR (yr^{-1})
IMF 6	3.2	0.15
IMF 7	5.0	0.23
IMF 7[a]	4.8	0.21
IMF 8	1.6	0.11
IMF 9	2.6	0.19
IMF 9[a]	2.8	0.21

[a] 25 million yr between bursts.

It is possible that some of the metals produced in the starburst are hidden, for example, by being blown out of the galaxy at very high temperature in the supernova-driven wind or by depletion onto interstellar grains. Nonetheless, models which do not overproduce metals by a large amount are to be favored over those which do. We have pursued this issue in the current models by including an estimate of the oxygen yields. The oxygen yield should increase monotonically as the starburst progresses. Table 6 shows the range of accumulated mass of oxygen at the time of observation for starbursts that were compatible with the other constraints.

Given a total mass of $2 \times 10^8\ M_\odot$ for the ISM, a solar abundance of oxygen would correspond to $1.3 \times 10^6\ M_\odot$. The bias toward very high mass stars in IMFs 6 and 7 leads to oxygen productions well in excess of this value, but IMFs 8 and 9 are probably consistent with observation (particularly if it is assumed that some of the oxygen is too hot to be detected via the far-infrared lines). The oxygen yields for all these models are relatively low because the double bursts yield less total oxygen than would long-duration bursts that came equally close to the other constraints.

When a massive ($>8\ M_\odot$) star completed its evolution, we assumed it always produced a supernova. Supernova rates at the time of observation are also included in Table 6. This table demonstrates that the oxygen production and supernova rate are nearly proportional to each other. Therefore, it is probably not correct to consider these two parameters as independent constraints. Nonetheless, it is noteworthy that the models based on IMFs 6 and 8 are the only two that have adequately low rates to be consistent with current estimates of the supernova rate.

The ability of the supernova rate to constrain the IMF is emphasized by Doane & Mathews (1993). Elements besides oxygen are also potentially useful. For example, neon has a well-measured abundance and is unlikely to be depleted onto grains. Its production is less strongly peaked toward massive stellar cores than is oxygen (Arnett 1978), so it would provide a slightly different constraint on the IMF than can be deduced from oxygen.

5.2. *The Bias in the IMF against Low-Mass Stars*

The conclusion from the modeling in § 4 is that it is very difficult to satisfy the constraints observed for M82 unless the proportion of low-mass stars is reduced compared with most proposed forms for the IMF in the solar neighborhood. The forms of the IMF proposed by Miller & Scalo (1979) and Rana (1987) allow models to approach the observations of M82 to within factors of 2 or 3 in critical parameters, but they still fall short by significant measures. The conflict is particularly dramatic if the local IMF resembles the forms proposed by either of these authors more recently, i.e., Scalo (1986) or the cases

analyzed by Basu & Rana (1992) which they feel are consistent with the observed number of white dwarfs.

Although we have used specific mathematical forms for the IMF for convenience in our modeling, the technique does not give significant insight to the required changes in the low-mass IMF other than the general statement that the proposed forms for the local IMF have too many low-mass stars to allow fits to the conditions observed in M82.

This conclusion is based on intentionally conservative observational and theoretical constraints. For example, the target for K flux was set at the observed lower limit, dereddening the galaxy under the assumption of a variable foreground screen of dust only and not allowing for optical depth effects (McLeod et al. 1993). We have modeled the CO index at the maximum strength allowed by the observations. The target UV flux is also a lower limit, based on the strength of the emission lines alone and carrying an assumption that the thick clouds of interstellar dust are ineffective in competing for ionizing radiation. Furthermore, in satisfying this constraint, we used stellar tracks that give a relatively high estimate of the UV outputs. The conservatism in setting the targets for UV and K flux is important because the models based on local IMFs had difficulty in matching even these lower limits. In attempting to fit these constraints, we also used an optimized SFR that is probably not fully achieved in the galaxy.

A class of uncertainty in this study arises from possible errors in the distance to M82. The dynamically determined mass goes as the first power of the distance, D, and the luminosities in the UV and near- and far-infrared go as D^2. Therefore, the luminosity-related constraints relax inversely with the distance to the galaxy. For example, the models plotted in Figure 2 would fit the observational constraints if M82 were only half as distant as we have assumed, i.e., were at 1.6 Mpc. Probably the most secure estimates of the distance to M82 are based on the distance to M81 plus the indications of a physical link between M81 and M82 (e.g., the bridge of intergalactic gas). Recent determinations of the distance to M81 based on Cepheid photometry (Freedman & Madore 1988) and measurements of planetary nebulae (Ford et al. 1989) give values of 3.3 and 3.4 Mpc, respectively, both in good agreement with the value of 3.2 Mpc we have assumed. The possibility of our constraints being relaxed significantly by an error in the assumed distance is therefore very remote.

Another possibility is that improvements in the stellar tracks could change the outputs of the starburst models in a way that would resolve the discrepancy between the observations and local IMF models. Here again, we have been conservative by selecting the family of tracks that give the highest estimate of the UV output. We have also shown that starburst modeling is robust against changes in the tracks, being only slightly affected even by the radical improvements that have occurred over the last 15 yr.

Finally, it is possible that some compromise IMF could be found that would be consistent both with the data on M82 and that on local star formation. However, we have shown that recent refinements in estimating the local IMF have moved it much further from the requirements to fit M82 than the version that was generally accepted 14 yr ago.

5.3. *The High-Mass IMF*

The IMF at high masses appears to have similar shape in a variety of environments (Freedman 1985). We have shown that the observations of M82 are compatible with a similar high-mass IMF, such as our IMFs 8, 9, 10, and 11, as well as with IMFs that fall less steeply toward high masses such as IMFs 6 and 7. The ability of IMFs 8–11 to meet the constraints in Table 4 would be enhanced by additional suppression of the formation of low-mass stars, although the supernova rates would be raised.

Can we distinguish between high-mass IMFs like those seen in other environments and those with an enhanced proportion of very high mass stars? From Table 6, it is interesting that models based on IMF 8 (which has a shape at the high-mass end that is similar to that observed in the solar neighborhood and in other environments) can meet or nearly meet the constraints discussed in the preceding section, produce a supernova rate near 0.1 yr^{-1}, within the observed range, and yield a mass of oxygen that will not greatly exceed solar abundances, assuming the ISM has a total mass of $\sim 2 \times 10^8\ M_\odot$ and that it was of low metallicity prior to the starburst. If is therefore plausible that the actual IMF in M82 is similar at the high-mass end to that in the solar neighborhood but has a reduced proportion of low-mass stars and an enhanced one of intermediate masses, similar in general form to IMF 8.

6. CONCLUSIONS

We used modern tracks of stellar evolution and a careful conversion to observable stellar parameters to generate starburst models. These models have been compared with the properties of the archetypical starburst in M82. Constraints on the models were set by a detailed reconsideration of the observational data for this galaxy (McLeod et al. 1993) and the rate of star formation was adjusted to optimize the fits. We find the following:

1. This type of model gives reliable results; relatively little change in the output parameters results from use of differing sets of theoretical tracks or from alternate methods of converting theoretical stellar parameters to observables.
2. The near-infrared spectrum of M82 is dominated by red supergiants, not by very metal rich red giants.
3. The properties of M82 cannot be fitted with starbursts based on any of the recently proposed forms for the local initial mass function.
4. The shape of the IMF for high-mass stars need not be different from that observed locally.
5. However, the predicted rate of supernova explosions with a local-type high-mass IMF is close to the maximum allowed by current observations—additional work in this area may further constrain the IMF in M82.
6. The low-mass portion of the IMF in M82 must be modified compared with local-type IMFs to suppress substantially the formation of stars with masses below a few $M_\odot$.

We appreciate helpful discussions with D. Arnett, R. Bell, R. Kennicutt, and R. Kurucz. J. Doane and W. Mathews communicated their work to us in advance of publication. A. Maeder kindly provided stellar evolutionary tracks in advance of publication. This work was supported by the National Science Foundation and by the Origins of Solar Systems program sponsored by NASA.

REFERENCES

Aaronson, M., Frogel, J. A., & Persson, S. E. 1978, ApJ, 220, 442
Arnett, W. D. 1978, ApJ, 219, 1008
Basu, S., & Rana, N. C. 1992, ApJ, 393, 373
Bell, R. A., & Briley, M. M. 1991, AJ, 102, 763
Bell, R. A., & Gustafson, B. 1989, MNRAS, 236, 653
Bernlohr, K. 1992, preprint
Bertelli, G., Bressan, A., Chiosi, C., & Angerer, K. 1986, A&AS, 66, 191
Chiosi, C., & Maeder, A. 1986, ARA&A, 24, 329
Doane, J. S., & Mathews, W. G. 1993, ApJ, submitted
Duffy, P. B., Erickson, E. F., Haas, M. R., & Houck, J. R. 1987, ApJ, 315, 68
Elias, J. H., Frogel, J. A., & Humphreys, R. M. 1985, ApJS, 57, 91
Flower, P. J. 1977, A&A, 54, 31
Ford, H. C., Ciardullo, R., Jacoby, G. H., & Hui, X. 1989, in IAU Symp. 131, Planetary Nebulae, ed. S. Torres-Peimbert (Dordrecht: Reidel), 335
Freedman, W. L. 1985, ApJ, 299, 74
Freedman, W. L., & Madore, B. F. 1988, ApJ, 332, L63
Frogel, J. A., Persson, S. E., Aaronson, M., & Matthews, K. 1978, ApJ, 220, 75
Gaffney, N. I., & Lester, D. F. 1992, preprint
Green, E. M. 1988, in Calibration of Stellar Ages, ed. A. G. D. Philip (Schenectady, N.Y.: Davis Press), 81
Green, E. M., Demarque, P., & King, C. R. 1987, The Revised Yale Isochrones and Luminosity Functions (New Haven: Yale Observatory)
Johnson, H. L. 1966, ARA&A, 4, 193
Kronberg, P. B., Biermann, P., & Schwab, F. R. 1985, ApJ, 291, 693
Kurucz, R. L. 1979, ApJS, 40, 1
Leitherer, C. 1990, ApJS, 73, 1
Maeder, A. 1992, private communication
Maeder, A., & Meynet, G. 1988, A&AS, 76, 411 (MM88)
McLeod, K. K., Rieke, G. H., Rieke, M. J., & Kelly, D. M. 1993, ApJ, 412, 111
Miller, G. E., & Scalo, J. M. 1979, ApJS, 54, 513
Panagia, N. 1973, AJ, 78, 929
Pottasch, S. R. 1984, Planetary Nebulae, A Study of Late Stages of Stellar Evolution (Dordrecht: Reidel)
Rana, N. C. 1987, A&A, 184, 104
Rieke, G. H. 1989, in Massive Stars in Starbursts, ed. C. Leitherer, N. Walborn, T. Heckman, & C. Norman (Cambridge: Cambridge Univ. Press), 205
Rieke, G. H., Lebofsky, M. J., Thompson, R. I., Low, F. J., & Tokunaga, A. T. 1980, ApJ, 238, 24 (RLTLT)
Scalo, J. M. 1986, Fund. Cosmic Phys., 11, 1
Schmidt-Kaler, T. 1982, in Landolt-Börnstein, Numerical Data and Functional Relationships in Science and Technology, ed. K. H. Hellwege, 22b, 453
Steiman-Cameron, T. Y., & Johnson, H. R. 1986, ApJ, 301, 868
VandenBerg, D. A., & Bell, R. A. 1985, ApJS, 58, 561